

Storm Tide Risk Assessment and High Resolution Modelling of Historic Tropical Cyclone Storm Tides in Nadi Bay, Fiji

26 May 2014

FINAL REPORT

Kathy McInnes and Ron Hoeke

Commonwealth Science and Industrial Research Organisation (CSIRO)

Table of Contents

| | |
|--|--|
| 1. Introduction | 3 |
| 2. Causes of Coastal Flooding..... | 3 |
| 3. Tropical Cyclone Storm tide Risk in Fiji..... | 5 |
| 4. Numerical Model Implementation..... | 7 |
| Archipelago Model | 8 |
| Nadi Model | 9 |
| Tropical Cyclones | 9 |
| 5. Model Validation | 10 |
| 6. Results | 13 |
| 7. Conclusions..... | 14 |
| 8. Recommendations..... | Error! Bookmark not defined. 15 |
| References | 16 |

1. Introduction

The Government of Australia through its Pacific-Australia Climate Change Science and Adaptation Planning (PACCSAP) Program is supporting a World Bank-funded project to undertake detailed floodplain modelling of the Nadi floodplain in Fiji. This support relates to the provision of information and model simulations of coastal sea levels along the Nadi coastline during tropical cyclones (TCs) at spatial resolutions that can inform detailed floodplain modelling.

Of the various types of weather systems that cause severe rainfall and flooding, TCs are particularly hazardous because of their potential to elevate coastal sea levels due to storm surges and high waves. In addition to causing flooding of low-lying coastal terrain, higher coastal sea levels during a storm surge can slow the drainage of floodwater from coastal river systems to the ocean. This in turn may worsen the severity and extent of coastal and upstream flooding by a process that is referred to as the 'backwater' effect.

This report is aimed at providing relevant information on TC-induced storm surges and coastal sea levels to inform the World Bank floodplain study. It summarises how the risk of these events may change under future climate scenarios and provides detailed hydrodynamic modelling of two recent TCs with a focus on the spatial variation of extreme sea levels along the Nadi coastline. Importantly, this high resolution modelling highlights uncertainties in extreme sea level predictions associated with large gaps in high resolution bathymetry and topography near shore.

2. Causes of Coastal Flooding

The main processes that lead to extreme sea levels and coastal flooding are described in Table 1. Along the west coast of Viti Levu, the most extreme sea levels are caused by TC-induced storm surge, when strong winds and low atmospheric surface pressure can significantly elevate coastal water levels. Together with astronomical tides, the elevated sea levels during a TC are called storm tides. The breaking of waves at the coast during such an event can further elevate coastal sea levels due to wave setup and runup (see Figure 1) and also cause coastal erosion. Wave breaking processes are highly localised and strongly dependent on coastal bathymetry and coastline orientation with respect to wave approach (Kennedy et al., 2012; Hoeke et al., 2013a). Tide gauges measure sea-level and are typically located in deeper water within sheltered harbours away from breaking waves so typically do not measure the larger sea levels at the open coast that occur due to wave setup and runup (see for example Hoeke et al, 2013a).

Storm surges are caused by the inverse barometer effect (IBE)¹ and surface wind stresses acting over coastal seas (wind setup). At the coast, TC-induced storm surges tend to be concentrated in the vicinity of maximum onshore winds close to the cyclone centre. The severity of storm surges is influenced by cyclone intensity and movement in relation to the impacted coastline. Coastal bathymetry also influences storm surges with wide and shallow continental shelf regions experiencing greater wind setup than narrow continental shelf regions and islands (e.g. Kennedy et al., 2012; Hoeke et al.,

¹ The inverse barometer effect describes the depression of the water surface under high atmospheric pressure, and its elevation under low atmospheric pressure.

2013a). Local coastal features such as peninsulas, offshore islands and reefs can shelter or focus the effects of wind and waves and cause local variations in coastal sea levels.

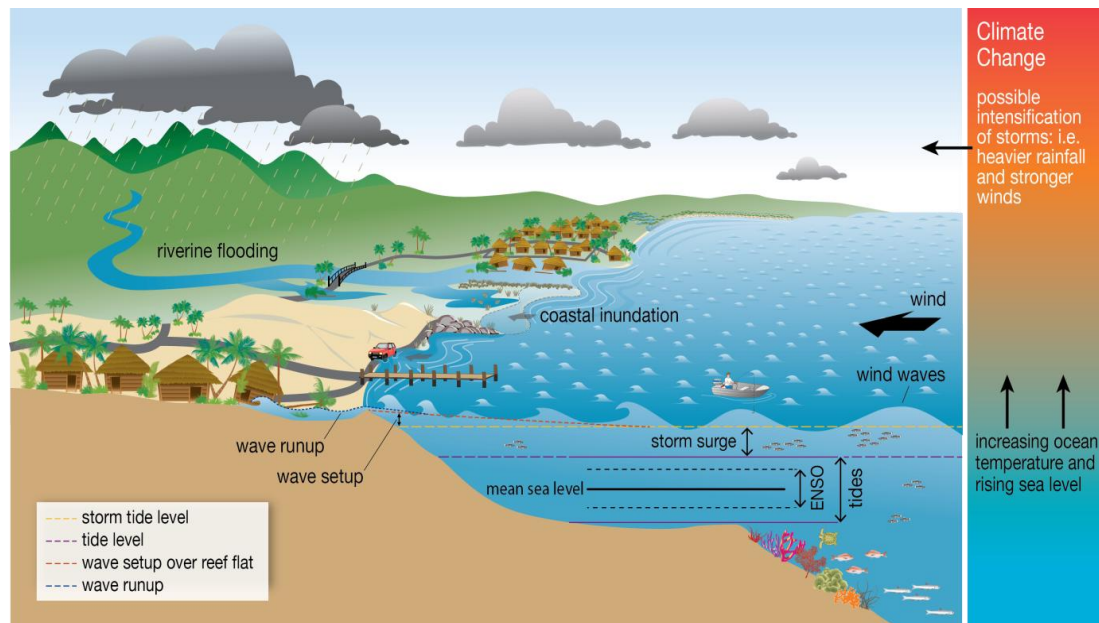


Figure 1: Foreground: the different processes that vary sea levels on daily, fortnightly and longer time scales due to tides and interannual variability such as ENSO. During storms, wind and falling pressure elevate sea levels to produce a storm surge while wind-waves breaking at the shore further elevate sea levels due to wave setup and runup. Background: elevated coastal sea levels can reduce river drainage and backed up water can worsen upstream flooding. Right panel: Climate change may impact processes in the system to worsen coastal flooding in the future through rising sea levels and possible intensification of storm systems which may increase storm surge height and rainfall during storms.

Sea levels can also be influenced by atmospheric and ocean processes that operate on longer timescales than a single storm. If these factors have a positive influence on sea levels (i.e. causing sea levels to be higher) at the time of a TC, they can worsen the extent of the coastal flooding and other associated impacts caused by the storm tide. These additional longer timescale sea level influences include long period astronomical tidal fluctuations that are described in Table 1. El Niño Southern Oscillation (ENSO) is also a major driver of such seasonal to interannual variability in the Pacific (Church et al., 2006; Walsh et al., 2012).

Storm tides can lead to flooding (inundation) of low-lying coastal terrain. The presence of higher sea levels at the coast can also worsen the severity and extent of flooding due to excess rainfall by slowing the rate at which rivers and streams can drain floodwater into the ocean. This process is referred to as the ‘backwater’ effect. For floodplain modelling, it is therefore of interest to consider the impact not only of rainfall from storm systems but also the coastal sea levels that may occur during such events. The purpose of this study is to provide information on coastal sea levels during TCs along the Nadi coastline for both historical and future climate conditions. Information from a recent Fiji-wide study (McInnes, et al. 2014) is revisited, with a focus on the Nadi Bay region. High-resolution modelling of the coastal sea levels associated with two recent historical TCs (Mick and Evan) is also undertaken to investigate the relationship between sea levels experienced in Nadi Bay and those measured at the tide gauge at

Lautoka and compare differences with the Fiji-wide model used in McInnes, et al. (2014) to inform a floodplain modelling study.

Table 1. Processes influencing actual sea level at the coast.

| Processes | Comments | Causes | Time Scale |
|--------------------------|--|--|-----------------------------|
| Wave run-up | The maximum height reached by individual waves on a coast | storms/swell | minutes to hours |
| Wave overtopping | The horizontal discharge of water over an obstacle | storms/swell | minutes to hours |
| Wave setup | time-averaged increase in water levels due to waves breaking | storms/swell | hours to days |
| Storm surge* | Rise in sea levels from Inverse Barometer Effect (IBE) and wind setup | Storms, e.g. tropical cyclones (TCs) | hours to days |
| Backwater | The presence of higher sea levels slowing the rate at which rivers and streams can drain floodwater into the ocean | Storms, e.g. tropical cyclones (TCs) | hours to days |
| Storm tide * | The combination of storm surge and astronomical tide | Storms/ planetary movement | |
| Astronomical tide | Normal tidal variations | planetary movement | days, weeks, seasons, years |
| Seasonal variations | | trade winds, ocean temperature | months to year |
| Interannual variations | Cycles in the climate on time scales of several years to decades | El Nino Southern Oscillation; Pacific Decadal Oscillation; | years to decades |
| Long-term sea level rise | | ocean thermal expansion/ ice melt | decades to centuries |

* Note that some definitions of storm surge and storm tide include wave setup but here wave setup is defined separately because of the need to additionally run wave models to estimate its contribution. Therefore our definition of storm tide = storm surge (i.e. IBE+wind setup) + astronomical tide.

3. Tropical Cyclone Storm tide Risk in Fiji

Statistical methods and Archipelago-scale coastal modelling were used in a recent study to estimate the Fiji-wide storm tide risks under late 20th Century 'baseline' conditions (defined as a 20-year period from 1980-2000), as well as 20-year future climate periods centred on years 2030, 2055 and 2090 (McInnes et al, 2014). TCs in the Fiji region over the period 1969-2007 were characterised in a statistical model that represented cyclone frequency, intensity and movement. The statistical model was then used to develop a population of random 'synthetic' cyclones and the simulated wind and pressure fields from these cyclones were used to force a hydrodynamic storm surge and tidal model for the baseline, 2030, 2055 and 2090 time periods. A map of the sea levels due to the combination of storm surge and astronomical tide, estimated to occur on average at least once every 100 years, is illustrated in Figure 2. These levels can also be viewed as having a 1% probability of being exceeded in any given year. The results indicate that storm tide risk is higher on the northwest coasts of both Viti Levu and Vanua Levu and lower on the southern and eastern coasts. This is because the northwest coasts face the direction from which TCs most commonly approach and because the ocean between the Yasawa group of islands and northwest coasts is shallower (less than 100 m deep), and therefore more favourable for the incidence of larger storm surges.

The impact of future sea level rise (SLR) and changes the frequency and intensity of TCs was also investigated. Sea level rise projections were presented in Australian Bureau of Meteorology and CSIRO (2011). For Fiji, sea levels are projected to increase between 0.1 and 0.3 m by 2055 and 0.16 to 0.62 m by 2090. The range of possible increases is because of the uncertainty in the amount of greenhouse gases that will be emitted in the future and because of uncertainty associated with the potential SLR for any given future emissions pathway.

Under future climate conditions, the TC frequency is projected to either remain the same or decrease slightly. However, the intensity of the most intense TCs is projected to increase. Changes to TC frequency and intensity were incorporated into the statistical model to represent future TC behaviour in Fiji. The changes consisted of a 25% reduction in TC frequency and a 10% increase in the intensity of maximum winds for the most intense cyclones.

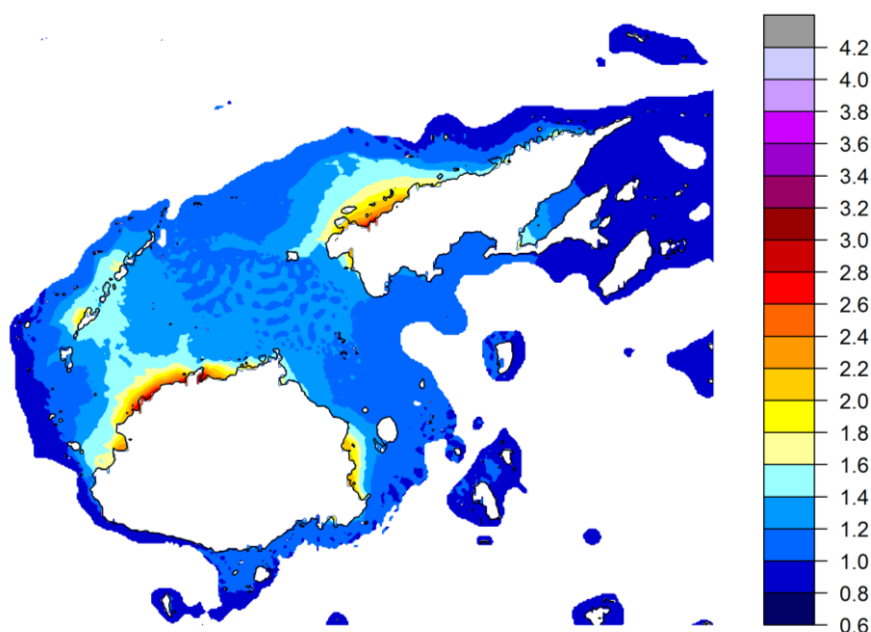


Figure 2 Modelled storm tide heights (m) corresponding with the 1-in-100 year storm tide during baseline (1980-2000) conditions.

Storm tide return intervals arising from the modelling are shown in Figure 3 and Table 2 for Lautoka and Nadi (note only the upper bound of the A1B SLR scenario for 2055 is used for ease of interpretation, see McInnes, et al. 2014 for further details). Under baseline conditions, these results indicate that there is little difference, on average, in storm tide risk between Lautoka and Nadi. It should be noted that these curves refer to TC-induced storm tides only. At shorter return periods (such as 20 years or less), other causes of extreme sea levels that include non-TC weather events, and which are not accounted for in this modelling, may also be important.

Projected SLR has a significant effect on extreme sea level return intervals: for instance, storm tide heights of approximately 2 metres – currently associated with a 1-in-100 year event – are projected to become more like a 1-in-50 year event (i.e. occur twice as often) by 2055 (Figure 3, Table 2). However, future changes in TC intensity (greater)

and frequency (fewer) leads to relatively small changes in future storm tide return intervals for shorter return period events. For instance considering SLR only, a 1-in-100 year storm tide is estimated to be 2.4 metres. If, in addition to SLR, projected changes to TCs are included, the storm tide height of a 1-in-100 year event remains similar. However, at longer return periods (i.e. greater than 1-in-200 years), the impact of more intense TCs becomes as important as SLR. For instance under present climate conditions, a storm tide height of 3 metres is associated with a 1-in-1000 year event. With sea level rise it will become a 1-in-500 year event (i.e. occur twice as often). If increased TC intensity is also considered, it becomes a 1-in-300 year event (i.e. occurs 3 times as often). But generally speaking, projected SLR is found to make the largest contribution to increased extreme sea level risk, as this increases the height of storm tides at all return intervals.

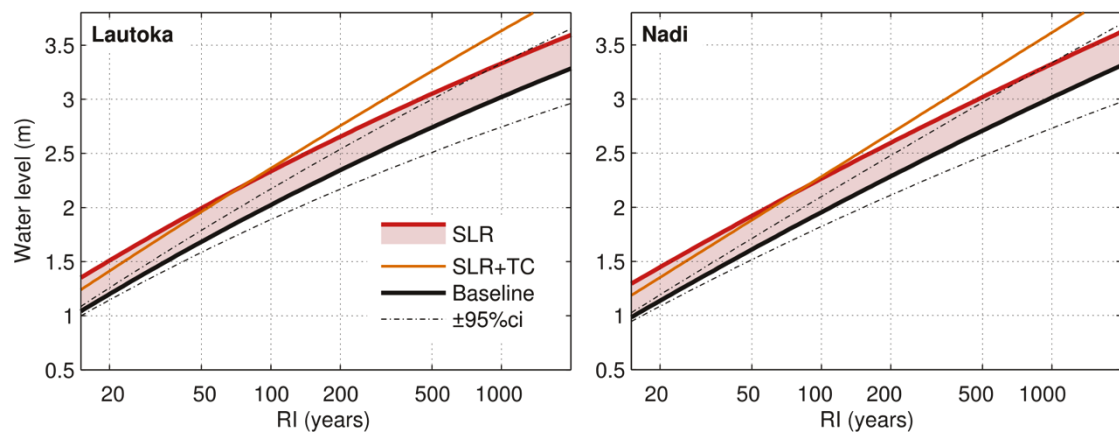


Figure 3. Return period curves for selected locations under the scenarios indicated in Table 4. 95% confidence intervals for the baseline scenario are also indicated with dashed lines. The shaded band represents the range of sea level rise (SLR) scenarios for 2055 added to the baseline (black) return levels, with the dark red line representing the uppermost scenario. The orange line represents return levels from the combination of changes TC frequency and intensity and the uppermost SLR.

Table 2. Estimates of storm tide heights (excluding effects of waves) for Lautoka and Nadi under baseline conditions; SLR conditions of 0.31 m (the upper uncertainty bound of emission scenario A1B in 2055); and SLR+ Δ TC conditions of SLR combined with a 10% increase in TC intensity and 25% decrease in frequency. See McInnes, et al. 2014 for further details.

| Location | Scenario | Sea level height | | | | | |
|----------|------------------|------------------|-------|--------|--------|--------|---------|
| | | 20-yr | 50-yr | 100-yr | 200-yr | 500-yr | 1000-yr |
| Lautoka | Baseline | 1.23 | 1.71 | 2.04 | 2.37 | 2.76 | 3.05 |
| | SLR | 1.54 | 2.02 | 2.35 | 2.68 | 3.07 | 3.36 |
| | SLR+ Δ TC | 1.43 | 1.99 | 2.38 | 2.77 | 3.27 | 3.66 |
| Nadi | Baseline | 1.15 | 1.64 | 1.97 | 2.30 | 2.73 | 3.04 |
| | SLR | 1.46 | 1.95 | 2.28 | 2.61 | 3.04 | 3.35 |
| | SLR+ Δ TC | 1.38 | 1.90 | 2.31 | 2.7 | 3.24 | 3.63 |

4. Numerical Model Implementation

Two Hydrodynamic models at different resolutions were used to simulate the historical impacts of TCs Mick and Evan and are named the 'Archipelago' model and the 'Nadi' Model. The Archipelago model is a Fiji-wide depth-averaged shallow water equations

model GCOM2D described in McInnes et al (2014), which covers the region from 15.2° - 20.2° S and 175.0° - 181.2° E at 1 km resolution. The Nadi model is the Delft3D hydrodynamic modelling system (Lesser et al. 2004; Roelvink and Banning 1994). The extent of the two models is provided in Figure 4.

Archipelago Model

Topographic and bathymetric data defining the region were obtained from General Bathymetric Chart of the Oceans (GEBCO) data on a global 30 arc-second grid available at <http://www.gebco.net>, which uses the 90 m Shuttle Radar Topography Mission data available at <http://srtm.csi.cgiar.org/> over land. Tide heights on the lateral boundaries of the hydrodynamic model were predicted using the tidal amplitudes and phases of the eight major tidal constituents (M2, N2, S2, K2, O1, K1, P1, Q1) obtained from a global tidal model (Le Provost et al., 1995).

Meteorological forcing for the hydrodynamic models is provided through the application of 10 m winds and mean sea level pressure obtained from the National Centres for Environmental Prediction Research (NCEP) Climate Forecast System Reanalyses (CFSR; Saha et al., 2010). These data are gridded globally at a horizontal resolution of ~38 km with hourly temporal resolution. Model simulations were performed firstly with CFSR data to investigate how well this gridded data set represented the cyclone. In the event that the CFSR data did not adequately resolve the wind or pressure forcing, an idealised cyclone model (Holland vortex) based on Holland (2008) was used to better define the wind and pressure field.

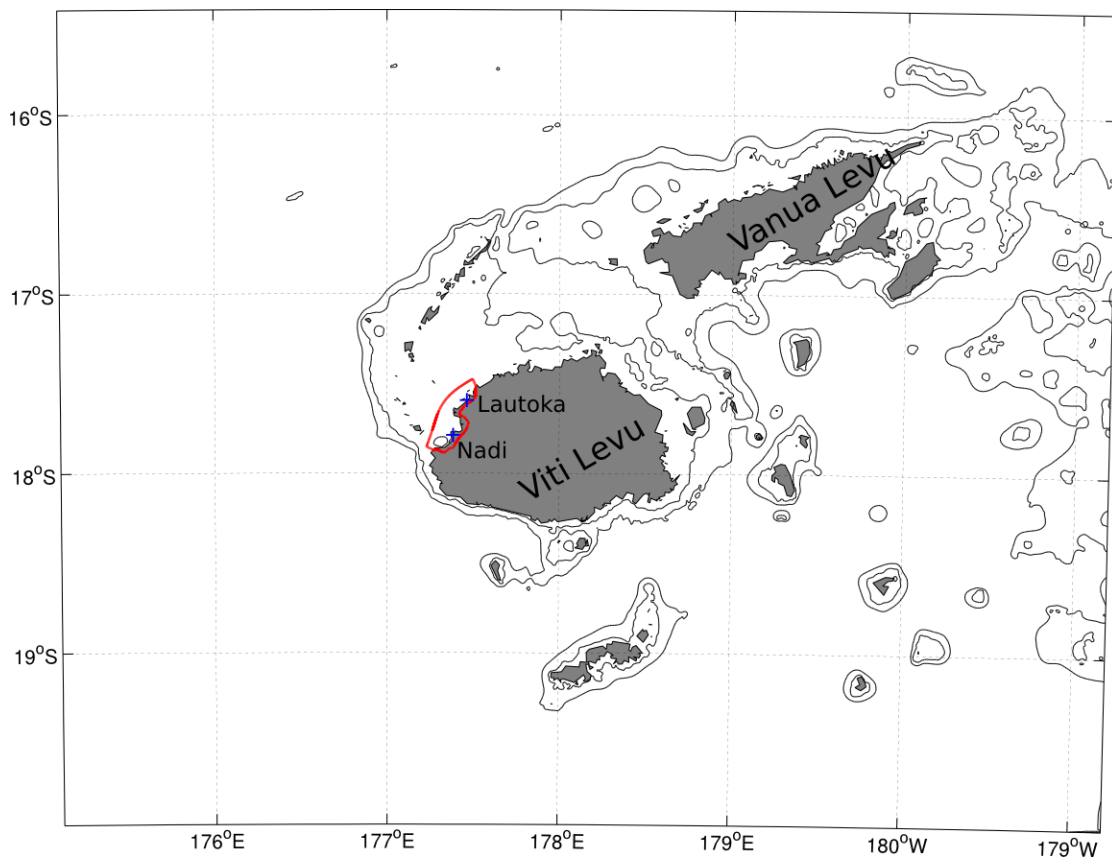


Figure 4. The boundary of the map represents the regional extent of the Achipelago Model. The Nadi Model's boundaries are shown in red.

Nadi Model

The Nadi model utilised the Delft3D flow module on a 2D curvilinear grid, which varied in spatial resolution from approximately 300 m near the ocean boundary down to approximately 25 m near the coast. The offshore water level boundary was forced by the Archipelago GCOM2D model run previously, interpolated along segments to the nearest output grid cells of the Archipelago model. The lateral boundaries were calculated as water-level gradients (Neumann boundary conditions); this allows the tides and storm surge to propagate along the offshore boundary while allowing water levels and current fields to adjust to both the offshore boundary water levels and other (wind and wave) forcing input at the lateral boundaries (Roelvink and Wasltra 2004). The same wind forcing was applied as for the Archipelago model, with winds interpolated to the Nadi model's grid.

Tropical Cyclones

Two TC events were investigated: TC Mick, which occurred in December 2009 and TC Evan which occurred in December 2012. The tracks of the two cyclones were obtained from the National Climate Centre of the Australian Bureau of Meteorology and are shown in Figure 5. Cyclone Mick followed a northwest-southeast path passing over the Yasawa islands, Lautoka and crossing Viti Levu to Suva. The main reported damage was to infrastructure. TC Evan travelled from the northeast down the west coast of Vanua Levu and Viti Levu elevating sea levels along the northwest coastline.

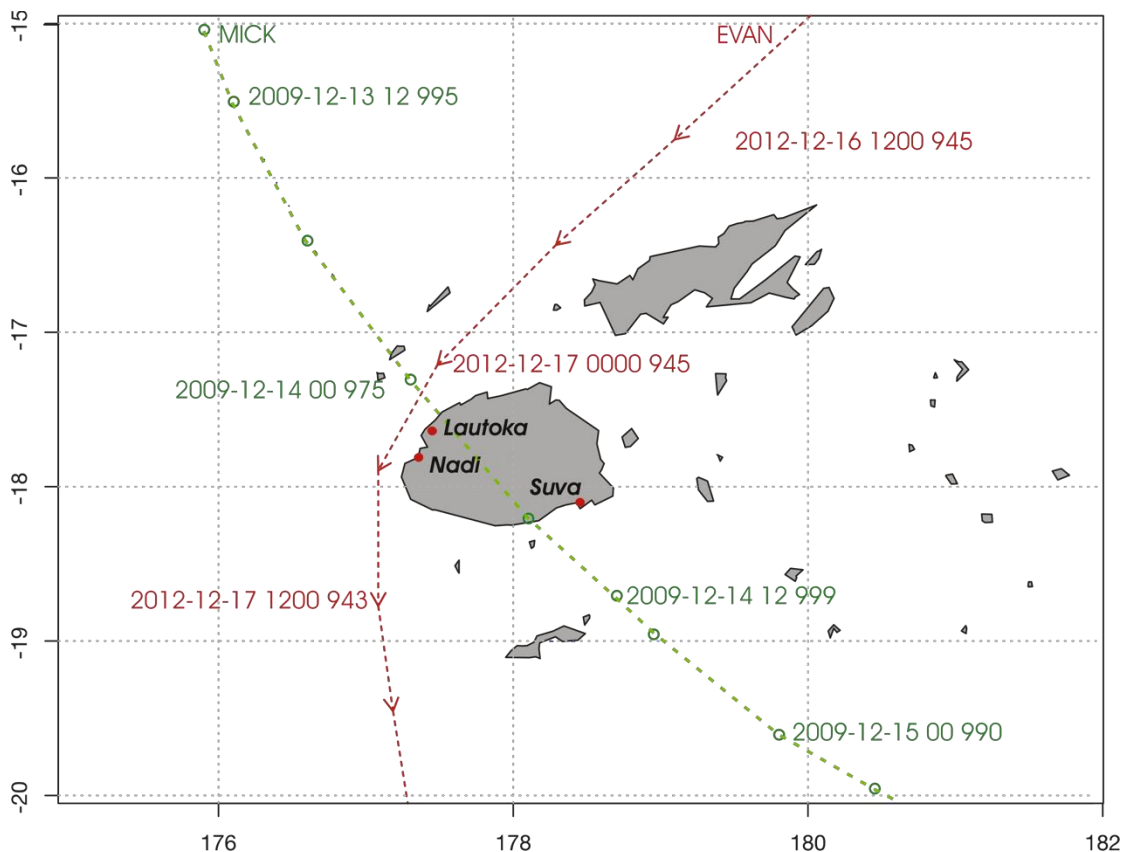


Figure 4 Best track data for TCs Mick (source: IBTrAKS) and Evan (source: Australian Bureau of Meteorology).

5. Model Validation

Modelled simulations of wind, pressure and sea level were compared with data from the Australian Bureau of Meteorology available for Lautoka tide gauge. Figures 5a and 5b compare the pressure, wind speed and direction from CFSR with that measured at the Lautoka tide gauge for TC Mick. Measurements indicated that the central pressure at Lautoka dropped to 970 hPa as the eye of the cyclone approached the gauge. The signature of the cyclone crossing is clearly seen in the wind speed and direction with winds from the northwest approaching, wind speeds diminishing in strength during the passage of the eye and then strengthening from the southwest following its passage. CFSR data for this case failed to identify the falling pressure and strengthening winds during the passage of this event. It was therefore decided to utilise the Holland vortex to better simulate the full intensity associated with the centre of the cyclone due to its close proximity to the coast. However, there are differences between the wind fields and the observations. Of particular note are the varied directions of the wind recorded by the anemometer. The CFSR winds indicate generally southeasterly winds ahead of the arrival of the cyclone centre compared to more easterly observed winds. The Holland vortex wind directions, while in closer agreement during the lead up to the arrival of the cyclone, indicates northwesterly winds following the cyclone whereas the observations indicated southwesterly winds.

Model simulations performed by the Archipelago model for TC Mick are shown in Figure 5c. These include a simulation with tides and weather forcing and one in which the tides have been removed through subtraction of a 'tide only' simulation. Prior to the arrival of the cyclone, close agreement with observations can be seen in the modelled tidal variations. However, in the simulation forced by CFSR winds and pressure, the model fails to simulate the variation in sea level during the passage of the cyclone. The use of a Holland vortex was investigated to better represent the wind and pressure variations due to the cyclone. Since the use of a Holland vortex requires the specification of a radius to maximum winds (RMW) for the cyclone and this information is not available within TC track databases such as IBTrACS, an assumption about the size of the cyclone was made based on an empirical relationship described in McInnes et al, (2014). Using this relationship led to values for the RMW that varied from about 35 to 45 km during its passage. When the Holland vortex forcing was applied, the peak of the storm surge was better captured in the model.

For TC Evan (Figure 6a and 6b) the pressure fall associated with the approach of the cyclone commences earlier in the CFSR data and is less pronounced than measured at Lautoka. Although the anemometer ceased functioning at around the arrival of the cyclone, the earlier commencement of the pressure fall in CFSR is accompanied by an earlier increase in the winds. The wind speed dropped off as the eye of the cyclone passed by. However the wind direction also differs between CFSR and observations. The observed winds are from the southwest whereas the observations indicate a southeasterly direction. For TC Evan, both Holland vortex and CFSR simulations produced storm surges higher than those actually measured – particularly using the Holland vortex – hence we used the CFSR data, which still overestimated storm surge but to a lesser extent than the Holland vortex.

Maximum water levels (storm tide heights) simulated by both the Archipelago and Nadi models were in excellent agreement with each other at the Lautoka tide gauge site: differences were 1-2 cm (Table 3). These simulated maximum levels differed from those observed by the tide gauge by 6-12 cm, and the timing of the simulated maximum storm tide height, as well as the maximum residual (the non-tidal component of storm tide),

generally occurred within 2.5 hours (usually much less) of those observed by the tide gauge. This indicates reasonably good agreement between simulated and observed maximum storm tides. Much larger differences between simulated and observed water levels (up to 30 cm) occur in the lead up to the storm tide peak during Evan, and to a much lesser extent during Mick. This is most likely due to the previously discussed differences in model wind fields. Patterns of maximum water levels and the implications of wind fields are considered in the following sections.

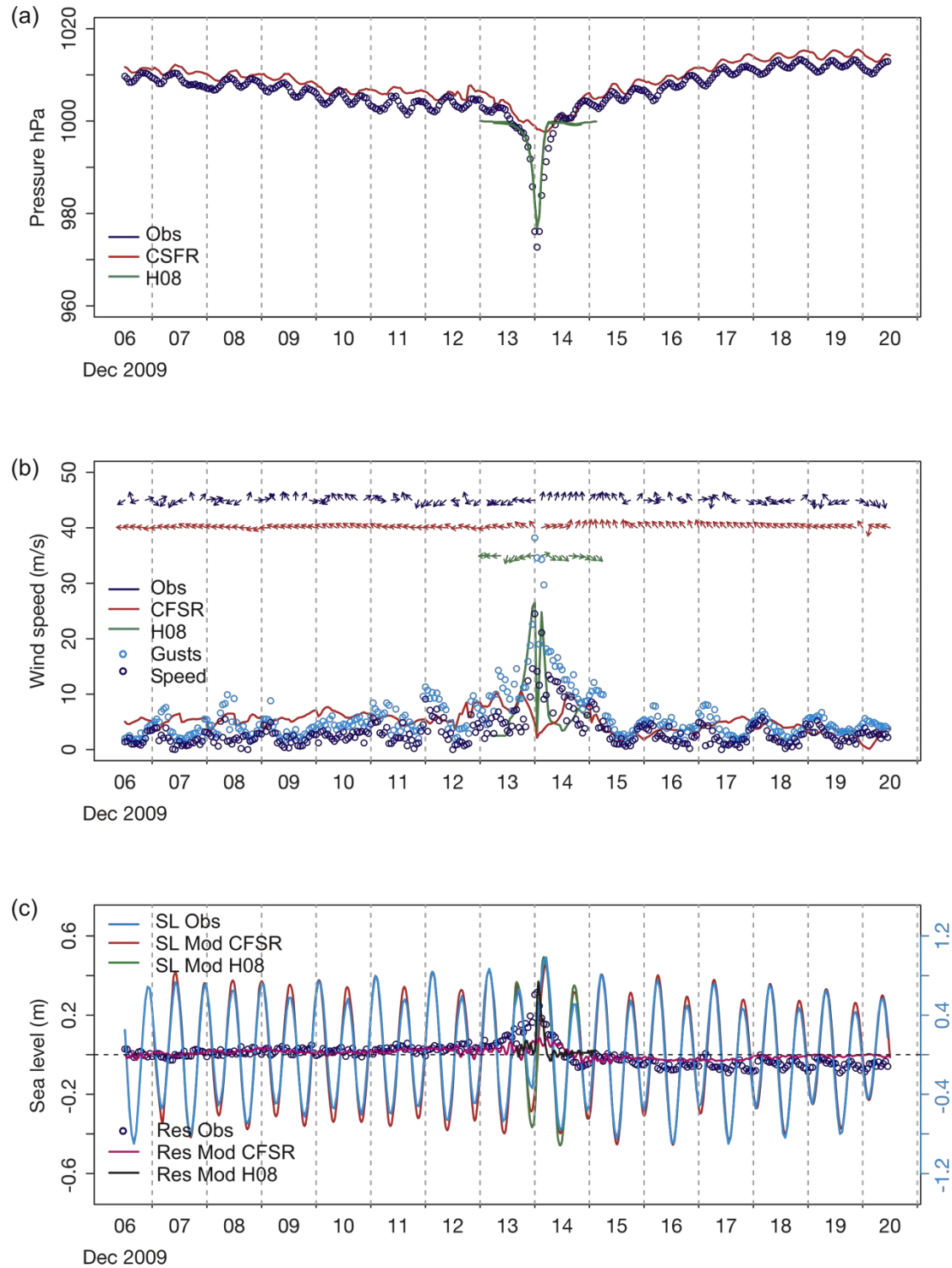


Figure 5 Time series for 15 days centred on TC Mick comparing observations, CFSR and Holland (2008) (a) pressure (b) wind speed and direction and (c) measured and modelled sea levels and sea level residuals.

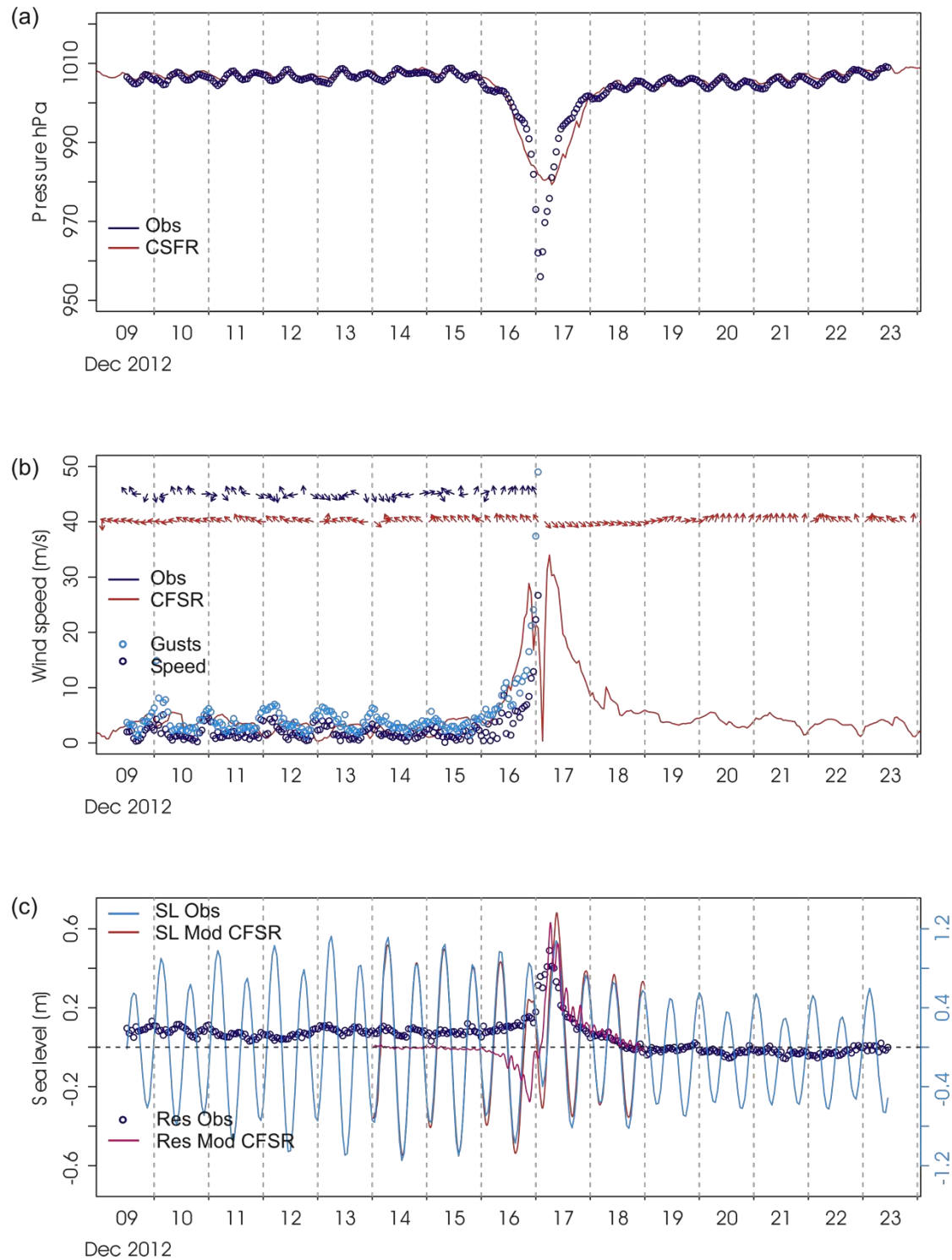


Figure 6 Time series for 15 days centred on TC Evan comparing observations and CFSR (a) pressure (b) wind speed and direction (note that the anemometer failed during the passage of this event) and (c) measured and modelled sea levels and sea level residuals.

6. Results

Simulated maximum storm tide heights at the Lautoka tide gauge were 1.02m and 1.04m for TC Mick and 1.29m and 1.28m for TC Evan, according to the Archipelago and Nadi models, respectively. These are levels roughly equivalent to the baseline 20-year return interval for both Lautoka and Nadi (Figure 3, Table 2), and maximum storm tide heights simulated by the Archipelago model differ little between Lautoka and Nadi (10cm and 4cm for Mick and Evan, respectively).

However, the Nadi model results show significantly greater variation in storm tide heights along the coast (Figure 7). For instance, simulated maximum storm tide heights were considerably lower (14cm less) at the Lautoka tide gauge than within Nadi Bay for TC Evan. The differences between Lautoka and the mouth of the Nadi River were smaller (10 cm for Mick, 1 cm for Evan), but maximum residuals were 26cm different for Mick, indicating that had Mick's storm surge occurred at a different stage of the tide, total storm tide would have been considerably different at the two locations. During TC Evan (which tracked more shore-parallel than Mick), the difference in maximum residuals between these two locations was only 3cm. Maximum water levels were 10-20cm higher within Nadi Bay compared to the Nadi River Mouth during both events. These results indicate that local differences in storm tides (in the order of 30cm) may occur between Nadi and Lautoka, but these differences are sensitive not only to TC characteristics such as track, forward speed and intensity, but also the timing of the stage of tide.

Table 3 - Maximum observed and simulated water levels (storm tide heights) and non-tidal residuals during TCs Mick and Evan for selected locations. White rows indicate values from the tide gauge; light grey from the Archipelago model; dark grey from the Nadi model.

| Cyclone | Site | Maximum water level (m) | Date, Time | Maximum residual (m) | Date, Time |
|---------|-------------------------------|-------------------------|------------|----------------------|------------|
| Mick | Lautoka tide gauge (observed) | 0.96 | 14/12,5:00 | 0.31 | 14/12,1:00 |
| | Lautoka | 1.02 | 13/12,3:00 | 0.45 | 14/12,0:30 |
| | Nadi | 0.92 | 13/12,3:40 | 0.22 | 14/12,1:50 |
| | Lautoka tide gauge | 1.04 | 14/12,3:20 | 0.38 | 14/12,1:50 |
| | Nadi Bay | 0.99 | 14/12,4:20 | 0.19 | 14/12,2:20 |
| | Denerau | 0.98 | 13/12,3:50 | 0.15 | 14/12,2:10 |
| | Nadi River Mouth | 0.94 | 14/12,3:40 | 0.12 | 14/12,2:10 |
| Evan | Lautoka tide gauge (observed) | 1.17 | 17/12,9:00 | 0.53 | 17/12,6:00 |
| | Lautoka | 1.29 | 17/12,9:00 | 0.63 | 17/12,5:40 |
| | Nadi | 1.25 | 17/12,9:30 | 0.49 | 17/12,9:30 |
| | Lautoka tide gauge | 1.28 | 17/12,9:10 | 0.38 | 17/12,8:50 |
| | Nadi Bay | 1.42 | 17/12,9:30 | 0.51 | 17/12,9:30 |
| | Denerau | 1.34 | 17/12,9:30 | 0.44 | 17/12,9:30 |
| | Nadi River Mouth | 1.27 | 17/12,9:20 | 0.36 | 17/12,9:10 |

Examination of Figures 4 and 7 illustrates how details of TC tracks and coastal topography and bathymetry can locally influence storm tide heights. As discussed in the previous sections, due to TC Mick's relatively shore-perpendicular track, crossing just

north-east of Lautoka, winds remained largely offshore, particularly south of Lautoka. This led to lower wind setup in the Nadi area relative to Lautoka. TC Evan, with its more shore-parallel track, caused onshore winds along the entire western side of Viti Levu, leading to generally more consistent storm tide levels along the coast (evident in the Nadi model results). In both of the historical cases, though, small geographical features led to localised ‘hotspots’ in the storm tide height simulations, e.g. Nadi Bay and Vaitogo Bay to the north-east of Lautoka.

The maximum water levels and non-tidal residuals simulated by both the Archipelago model and the Nadi model at the Lautoka tide gauge site are generally in very good agreement with the tide gauge observations, with differences generally less than 10 cm. However, some details of the simulated water level history do depart from observations. In particular, there is noticeable set-down (negative residuals) in the simulated results for Evan not visible in the observations (Figure 6c). This corresponds to a period of strong offshore-directed model winds; observed winds are not as strong or as offshore-directed (Figure 6b). This strongly suggests local topography (i.e. the hills and mountains neighbouring Nadi and Lautoka) affects the local wind fields in ways not captured by either the CSFR or Holland winds used by both models, which in turn limits the robustness of the simulated storm tide results.

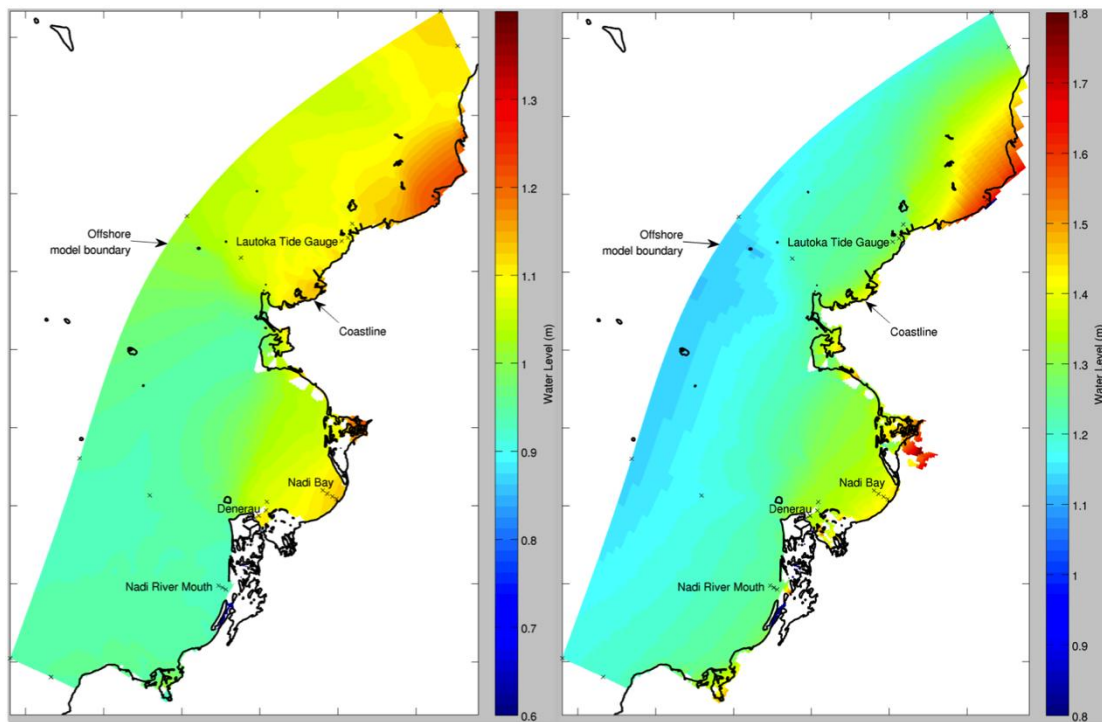


Figure 7 – Maximum storm tide heights simulated by the Nadi model for Cyclone Mick (left) and Cyclone Evan (right). Note the colour scale of the two plots is different. The labeled locations near the coastline indicate the locations listed in Table 2.

7. Conclusions and Recommendations

The archipelago model and the much higher spatial resolution Nadi model produced broadly similar maximum storm tide heights for historical TCs Mick and Evan, in good agreement with observations at the Lautoka tide gauge. The Nadi model also produced relatively large local differences (variation) in storm tides and associated residual water

levels along the coastline during the two storms, i.e. up to 26 cm between the location of the Lautoka tide gauge and the mouth of the Nadi River in the case of Mick. There were also similar differences between Nadi Bay and other locations within the Nadi model domain (Figure 7). It should not be discounted that still larger alongshore differences in storm tide heights during any particular TC (past or future) are possible. Hence storm tide levels in Nadi Bay or Nadi River or elsewhere along the western coast of Viti Levu should not be assumed to be the same as indicated by the Lautoka tide gauge. Fluvial (river) flooding studies, such as currently underway for the Nadi River watershed, should therefore use caution before basing storm tide heights at their seaward boundary off nearby tide gauge information.

Reasons for this local variation in storm tide heights are twofold: first, a particular TC's track, forward speed and tight radius of winds lead to local variations in the timing and magnitude of storm surge along the coast; second, local bathymetry and topography interact with the TC's wind field, changing both the wind field itself (topographic effects) and the TC's coastal currents (bathymetric effects), which redistributes wind setup along the coast. These bathymetric effects highlight the importance of small-scale features such as peninsulas, islets and reefs to local inundation risk.

The sensitivity of the Nadi model to small-scale coastal features leads to an important caveat. Very little high-resolution bathymetry and topography was available to inform the Nadi model: large swathes of the area covered by the model contain no local bathymetric information at all and so values were interpolated from low resolution sources of bathymetry data (GEBCO). It is therefore likely that multiple bathymetric features (reefs, sand bars, etc.) are absent in the model, leading to very low confidence in the quantitative details of the predicted storm tide variation along the coast. This lack of available bathymetric information also made direct simulation of wind-waves impossible, since wave propagation and dissipation in coral reef environments (such as those surrounding Viti Levu) are especially sensitive to small-scale bathymetric features. Without knowledge of both offshore and nearshore bathymetry, quantitative estimates of wave setup and run-up – which could further exacerbate coastal flooding (e.g. Hoeke, et al. 2013b) are not possible. Indeed, any risk analysis of storm tides based on numerical modelling at the spatial scales of the Nadi model (or higher) is of questionable integrity, without the requisite morphological information.

Future storm tide risk analysis for the Nadi Bay region (or elsewhere in Fiji) should include a concerted effort to collate existing sources of bathymetry and topography, identify where such data is absent or insufficient, and prioritise efforts to collect data in missing areas. Such data would also allow for higher resolution wind field models which can take into account the topographic effects discussed above. Validation of storm tide heights at locations other than the Lautoka tide gauge would also greatly improve model accuracy. This could be implemented with a relatively low-cost network of pressure sensors. The accuracy of both coastal and terrestrial (fluvial) inundation risk relies on the quality of underlying geophysical data. Investment in the collection of topographic and bathymetric datasets and in situ physical observations (e.g. water levels, waves, winds and precipitation) provides greater confidence in risk assessments and potential impacts, allowing for more efficient infrastructure design and greater resilience.

References

- Australian Bureau of Meteorology and CSIRO. 2011. Climate Change in the Pacific: Scientific Assessment and New Research. Volume 1: Regional Overview. Volume 2: Country Reports, 530 pp.
- Church, J. A., White, N.J., Hunter, J.R., 2006. Sea-level rise at tropical Pacific and Indian Ocean islands. *Global and Planetary Change* 53, 155-168.
- Hoeke, R.K., McInnes, K.L., Kruger, J., McNaught, R., Hunter, J., Smithers, S., 2013a. Widespread inundation of Pacific islands by distant-source wind-waves. *108*, 128–138.
- Hoeke, R.K., McInnes, K.L. O’Grady, J.G., Lipkin, F., Colberg, F. 2013b: High resolution Met-Ocean modelling for storm surge risk analysis in Apia, Samoa. Report prepared for Australian Department of Environment, 66 pp.
- Holland, G., 2008. A revised hurricane pressure–wind model. *Monthly Weather Review* 136, 3432-3445.
- Kennedy, A. B., et al., 2012. Tropical cyclone inundation potential on the Hawaiian Islands of Oahu and Kaua., *Ocean Modelling* 52–53, 54-68.
- Le Provost, C., Genco, M.L., Lyard, F., 1995. Modeling and predicting tides over the World Ocean." *Quantitative skill assessment for coastal ocean models (1995)*: 175-201.
- Lesser, G. R., Roelvink, J. A., van Kester, J. A. T. M., Stelling, G. S., 2004. Development and validation of a three-dimensional morphological model, *Coastal Engineering*, 51(8-9), 883-915.
- McInnes, K.L, Walsh, K.J.E., O’Grady, J.G., Hoeke, R.K., Colberg, F. and Hubbert, G.D. 2014: Quantifying Storm Tide Risk in Fiji due to Climate Variability and Change. *Global and Planetary Change*. 116: 115–129.
- Roelvink, J. A., Waslra, D. J., 2004. Keeping in simple by using complex models, in 6th International Conference on Hydroscience and Engineering, *Advances in Hydro-Science and Engineering*, edited, Brisbane, Australia., Brisbane, Australia.
- Walsh, K. J. E., McInnes, K.L., McBride, J.L., 2012. Climate change impacts on tropical cyclones and extreme sea levels in the South Pacific — A regional assessment. *Global and Planetary Change* 80–81, 149-164.